Linear Polarization to Circular Polarization Conversion Metasurface Antenna for X Band application

Vishnu D [a] , T A Shahul Hameed[b], Sheeba O[c]

a) *Research Scholar, LBS Centre for Science and Technology. University of Kerala*
b) *Professor, Department of ECE, TKM College of Engineering, Kollam*
c) *Rtd. Professor, Department of ECE, TKM College of Engineering, Kollam*

***Abstract*—**A reconfigurable antenna employing a Complementary Metasurface for polarization adjustments is introduced, with a Slot antenna serving as the primary radiating component. The Complementary Metasurface Structures, derived from the Babinet Principle and the Principle of duality applied to conventional structures, are utilized. A unit cell featuring a zig-zag geometry is employed to construct the meta-surface, contributing to a significant reduction in size. By rotating the Metasurface structure above the radiating element, the antenna achieves Linear Polarization (LP) to Circular Polarization (CP) conversion within the 7GHz to 9GHz frequency range. This conversion holds practical applications in satellite communication, Wi-Fi devices, radar systems, and more.

***Index Terms*— Polarization, Frequency, Reconfigurable antenna, Metasurface, Metamaterial**

Introduction

In wireless communication systems, antennas are indispensable. The demands of contemporary wireless communication necessitate compact antennas with improved performance, versatile functionality, higher gain, and a reduced size [1]. Substituting multiple discrete antenna structures with a single, compact, and reconfigurable antenna structure proves beneficial in wireless communication systems. Reconfigurable antennas are generally categorized into three main types: Frequency [2, 3], radiation pattern [4], and polarization [5, 6] reconfigurable antennas.

Hybrid or compound reconfigurable antennas find common use in scenarios where more than one parameter of the antenna requires adjustment. The reconfiguration of polarization and frequency can be accomplished through electrical or mechanical means [7, 8]. Preference is given to electrical-based reconfiguration over mechanical methods. Historically, methods involving the use of PIN diodes, varactor diodes [26, 27], and parasitic pixel layers were widely employed for reconfiguration. However, a notable drawback of these methods is the need for additional biasing elements, leading to increased bulk. Recently, structures like metasurfaces have been introduced, enabling polarization reconfiguration [9] and frequency reconfiguration [10, 11] without the necessity of extra biasing elements. The metasurface, characterized by a distribution of electrically small scatters and often termed a two-dimensional metamaterial, has gained significant popularity in reconfigurable antennas. This is primarily due to its compact design and cost-effectiveness. The utilization of metasurfaces eliminates the need for biasing elements and additional power sources. In a study by H. Zhu et al. [12], a polarization reconfigurable antenna was proposed, featuring a metasurface positioned atop the main radiating antenna. This configuration enables the realization of linear polarization, right-hand circular polarization, and left-hand circular polarization through the rotation of the metasurface. In the works [10, 13-17], a series of frequency reconfigurable antennas were introduced, featuring reconfigurability achieved through the rotation of a metasurface positioned atop the antenna. Rachedi, K et al. [45] proposed a compact reconfigurable antenna designed for Green Wireless Communication, exhibiting the capability to generate up to eight radiation patterns. T. Cai et al. [18] presented an X-band quad-beam transmits array utilizing an enhanced dual-mode metasurface, achieving a full phase circle of 360 degrees. Additionally, H. X. Xu et al. [19] proposed a bifunctional metasurface designed to efficiently control radiation beams. Metasurfaces are commonly employed as polarizers in these applications. C. Fang et al. [20] and J. C. Zhao et al. [21] introduced a wideband and ultra-broadband reflective LP converter known for its high efficiency. In a separate work, Sam, W et al. [44] designed and manufactured a reconfigurable integrated SIW filter and antenna employing varactor diodes. The reconfigurability was achieved through a multi-layer technique and the application of reverse voltage to turn the filter. J. Zhao et al. [22] proposed an enhanced photo-excited switchable broadband reflective LP conversion metasurface designed for Terahertz (THz) waves. This proposed structure attained a 99% PCR value for resonance frequencies at 1.42 THz, 1.01 THz, and 0.69 THz. G. Varamini et al. [23] proposed a structure in which metamaterial was overloaded on a microstrip antenna, allowing the antenna to efficiently acquire dual-band characteristics. Additionally, G. Varamini et al. [24] presented a microstrip antenna based on loop formation and a metamaterial load, achieving circular polarization by altering the current distribution through changing the position of the metasurface. In another contribution, H.-X. Xu et al. [25] proposed a multifunctional microstrip array utilizing a linear polarizer and a focusing metasurface.

In the work by Alnahwi et al. [41], a novel sensing and communicating antenna for Cognitive Radio (CR) systems is

presented. The communicating antenna is designed as a frequency-reconfigurable antenna using a varactor diode attached to the radiating patch. The mutual coupling between the sensing and communicating antenna is reported to be less than -20dB. Shankarappa S. et al. [42] developed a pattern-reconfigurable antenna aimed at establishing an intersatellite communication link between flying spacecraft. PIN diodes are utilized to select Reconfigurable Selective Reflectors (RSR), and the antenna resonates at 2.45 GHz, exhibiting good impedance matching and a wide beam width. Ahmed.S et al. [43] investigated the introduction of metasurfaces in a filtering antenna. The studies concluded that a filtering antenna designed using metasurfaces is efficient for radar systems, medical monitoring, and firefighter tracking.

Slot Antenna Design

Slot antenna serves as the basic radiating element.

Slot antenna is an opening cut in a conductor sheet. The slot antenna is the complement of the dipole antenna. The principle of duality and babinet can be applied to slot and dipole structures .Compared to dipole slot is preferred for longer distance communication, enhanced impedance matching and high mechanical stability.

$$Z_{SC}Z_{S}=\eta^2/4$$

where Z_{SC} is the impedance of dipole antenna which is 73+j42.5 and η represents the free space impedance which is 377Ω. On calculating we get the value of Z_S the impedance of slot as 363-j211 solving for real part the impedance will 486 Ω which provide excellent matching with free space. Slot antenna can be designed for various frequency bands depending on the length and width of the slot. Here two slots are cut to obtain two resonating frequencies, the spacing between the slots, width and length of the slots determine the resonating frequency. The feed line is fed symmetrical with respect to the centre. The slot antenna produces linearly polarized waves.

Slot antennas can be designed for various frequency bands by adjusting the length and width of the slot. Introducing two slots enables the attainment of two resonating frequencies, with the spacing, width, and length of the slots determining these frequencies. The feed line is symmetrically connected with respect to the center. Additionally, slot antennas generate linearly polarized waves. The resonant frequency of slot antenna can be calculated as

$$f_r = \frac{c}{2L}$$

c represent speed of light, L represent length of slot. The width of the antenna is an important parameter determining the impedance of antenna. The width and input impedance of the antenna is related as,

$$Z_{in} = \frac{120\,W}{\sqrt{\epsilon_r}\;L}$$

The outcomes of the simulation depicted in Figure 1 indicate that the slot antenna designed exhibits resonance within the 7 GHz to 12 GHz range, with peak resonance occurring at frequencies of 9.1 GHz and 11.1 GHz due to the presence of two slots. The structure exhibits an axial ratio exceeding 40 dB Figure2. across the frequency range of 7 GHz to 12 GHz, thereby verifying the linear polarization of the slot antenna.

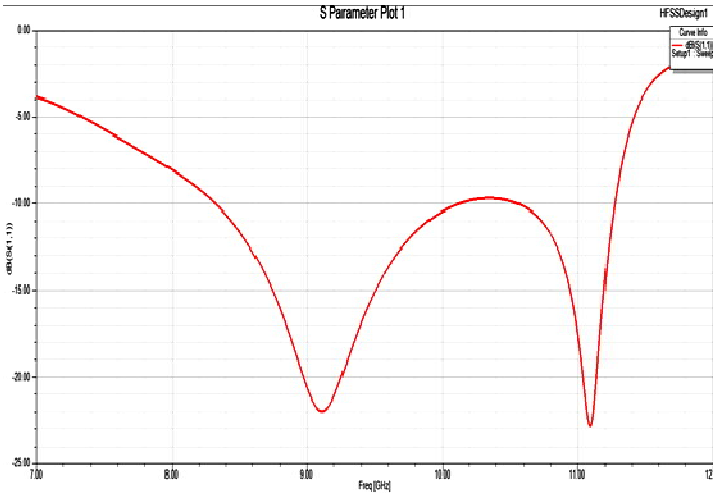

Figure 1. Slot antenna S_{11} parameter

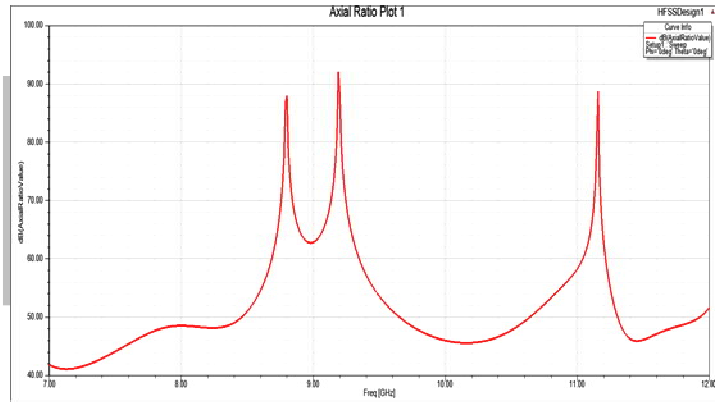

Figure 2. shows the axial ratio plot in db scale in the frequency range 7 GHz to 12 Ghz. Over this range of frequency the slot antenna is providing linear polarization.

Metasurface for Polarization reconfiguration

The metasurface utilized in this study is the complementary structure of the unit cell proposed by [45]. The primary radiating element emits a linearly polarized wave. Introducing a Zigzag-shaped metasurface causes the linearly polarized wave's electric field vector to decompose into two orthogonal components:

$$E = E_x + E_y$$

The metasurface structure can be represented equivalently by an RLC circuit, the E_x and E_y components provides different impedances Z_1 and Z_2 along the unit cell structure . Z_1 and Z_2 are complex impedances represented by the resistive part and reactive part contributed by the Resistance and Capacitor and inductor of the RLC.

Since Z_1 and Z_2 are complex impedances it can be represented as

$$Z_1 = |Z_1|\angle Z_1$$

and $Z_2 = |Z_2|\angle Z_2$

If the geometry of the metasurface is arranged in such a manner that $|Z_1| = |Z_2|$ and $\angle Z_1 - \angle Z_2 = 90^0$ then $|E_x| = |E_y|$ and $\angle E_x - \angle E_y = m\pi$ which result in linear polarization , m represent an integer

Similarly, if the geometry of the metasurface is arranged in such a manner that $|Z_1| = |Z_2|$ and $\angle Z_1 - \angle Z_2 = 90^0$ then $|E_x| = |E_y|$ and $\angle E_x - \angle E_y = n\pi$ which result in circular polarization, n represent an integer.
In this work a metasurface structure is placed above the slot antenna and rotated to get the condition of linear and circular polarization. The simulation is done in HFSS. The simulation results are explained in the coming parts.

Linear Polarization

Linear polarization is a characteristic of electromagnetic waves in which the electric field vector oscillates in a straight line along a specific direction as the wave propagates through space. The oscillation remains along a constant plane, and the direction of this plane determines the polarization of the wave. The Electric field of a linearly polarized wave can be represented as

$$E(z,t) = E_0 \cos(kz - \omega t + \theta)\mathrm{a_x}$$

The design of a meta-surface for linear polarization involves manipulating the phase response of the surface to achieve the desired polarization state. The equations governing this design are often related to the geometric and electromagnetic properties of the meta-surface. For linear polarization conversion, the meta-surface should introduce a specific phase shift between the horizontal and vertical polarization components represented by

$$\emptyset = \frac{2\pi}{\lambda}(d + \Delta n.h)$$

Where, ϕ is the phase shift, λ is the wavelength , d is the thickness of the meta-surface, Δn is the birefringence of the meta-surface material is a key factor in achieving differential phase shifts for different polarizations h is the height of the meta-surface structure. The relationship between incident and transmitted electric field from in the metasurface is related using Johns Matrix(J).

$$E_{out} = J\,E_{in}$$

E_{out} and E_{in} represent the incident and transmitted Electric field and J represent the Johns Matrix.
In case of linear polarization

$$J = \begin{bmatrix} \cos(\emptyset) & \sin(\emptyset) \\ \sin(\emptyset) & -\cos(\emptyset) \end{bmatrix}$$

The axial ratio is a parameter used to quantify the polarization of electromagnetic wave, particularly in the context of antennas. The axial ratio is defined as the ratio of the major axis to the minor axis of the polarization ellipse. For circular polarization, the polarization ellipse degenerates into a circle, and the axial ratio is defined as the ratio of the maximum to the minimum amplitude of the electric field in one cycle of the wave. Figure 4 displays the S11 parameter corresponding to the configuration illustrated in Figure 3, indicating resonance of the antenna at 8.75 GHz. In Figure 5, the axial ratio plot demonstrates that at 8.75 GHz, the axial ratio in decibels is approximately 50, providing justification for the linear polarization.

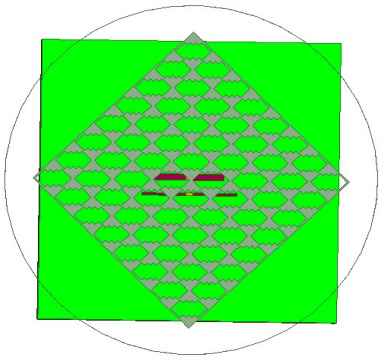

Figure 3. Metasurface alignment to obtain linear polarization

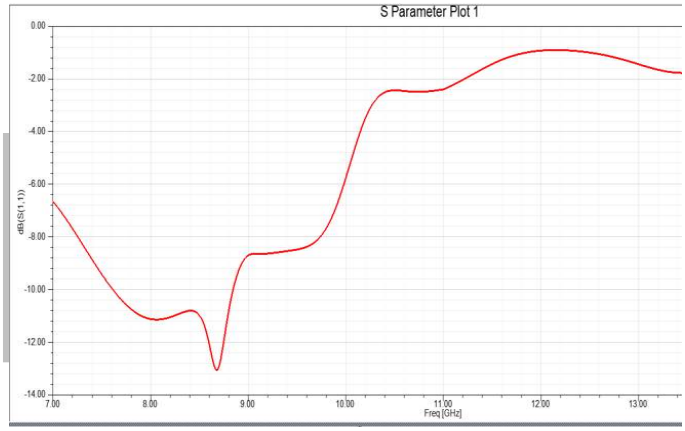

Figure 4. S_{11} plot for linear polarization

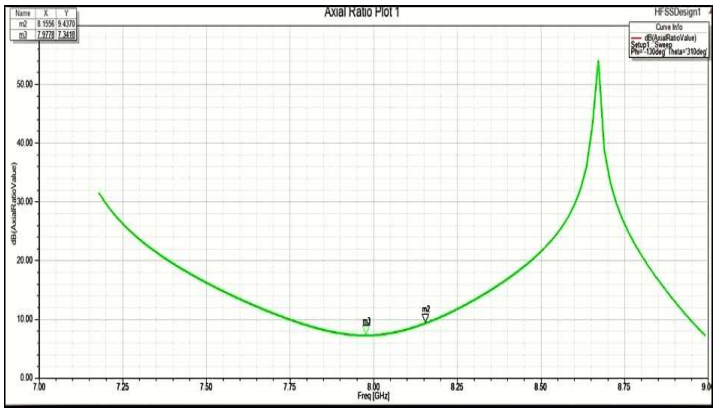

Figure 5. Axial Ratio plot for linear polarization

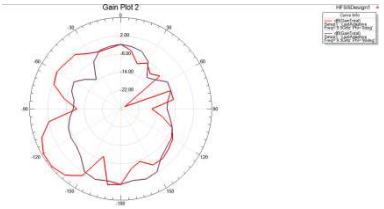

Figure 6. Gain plot for Linear polarization

Circular Polarization

Circular polarization in described using complex phasors. Circular polarization can be right-handed (clockwise) or left-handed (counterclockwise), and it is characterized by the rotation of the electric field vector as the wave propagates.
For a right-handed circularly polarized wave, the electric field vector

$$E+= \frac{1}{\sqrt{2}} (X + iY)E_0 \, e^{i(kz-\omega t)}$$

For a left-handed circularly polarized wave,

$$E-= \frac{1}{\sqrt{2}} (X - iY)E_0 \, e^{i(kz-\omega t)}$$

E_0 Amplitude of the Electric Field
k wave number
z Direction of Propagation of Wave
X and Y represent the vectors in x and y direction
ω Angular Frequency

Circular polarization can be achieved using metasurfaces by tailoring the phase and amplitude of the transmitted wave by the slot antenna. A widely used method for generating circular polarization using a metasurface employs subwavelength resonators or elements arranged in a particular pattern. These elements are strategically designed to introduce a spatial phase shift of π/2 between the components of the electric field, achieving the desired polarization state. Additionally, the amplitudes of these components are adjusted to ensure equal amplitudes, contributing to the overall circular polarization effect. Design process and specific parameters for achieving circular polarization with a metasurface can be complex and application-specific. Numerical simulation tools like HFSS and optimization techniques are often employed in the design process to achieve the desired polarization characteristics it is necessary to calculate the phase difference between x-polarized and y-polarized wave as

$$\Delta\emptyset = \emptyset(t_y) - \emptyset(t_x)$$

where $\emptyset(t_y)$ and $\emptyset(t_x)$ are the phase angles of the complex transmission coefficients for x-and y-polarized incident fields. In the case of an incident linearly polarized wave with a polarization angle $\emptyset_0 = \pi/4$ with respect to x-axis, the electric field components along different axes are equal as $E_{in}c,x = E_{in}c,y$. When the designed surface can lead to $\Delta\Phi = \pi/2$ and Tx/Ty = 1, the transmitted wave is thus transformed into right circular polarized (RCP) light while $\Delta\Phi = -\pi/2$ and Tx/Ty = 1, a left circular polarized light (LCP) is obtained. To combine both conditions on transmitted amplitude and phase together, we can define a single parameter as criterion for polarization conversion rate.

The axial ratio is a parameter used to quantify the polarization of electromagnetic wave, particularly in the context of antennas. The axial ratio is defined as the ratio of the major axis to the minor axis of the polarization ellipse. For circular polarization, the polarization ellipse degenerates into a circle, and the axial ratio is defined as the ratio of the maximum to the minimum amplitude of the electric field in one cycle of the wave.
Examining the S_{11} graph in Figure 8, it is determined that the resonant frequency is 8.3 GHz. Additionally, the axial ratio plot Figure 9. reveals that it tends towards zero at this resonating frequency, providing evidence that the structure manifests a circular polarization state.

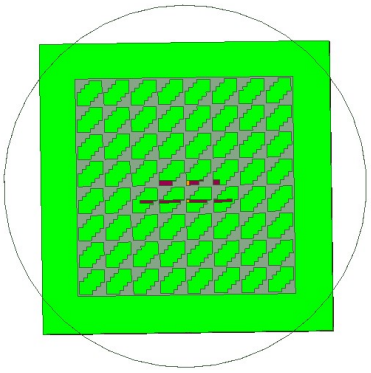

Figure7. Metasurface alignment to obtain circular polarization state

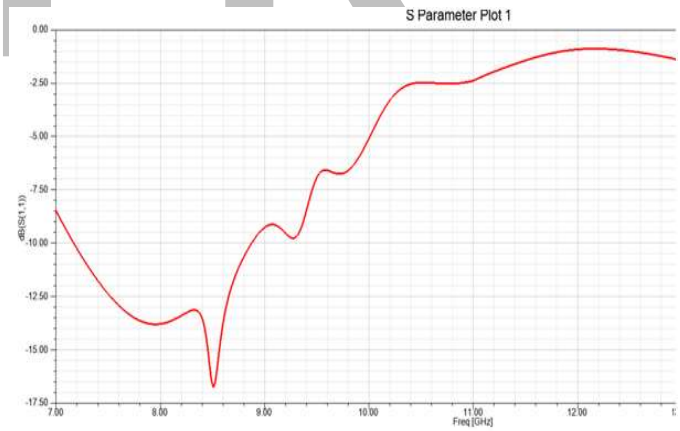

Figure 8. S11 plot in case of circular polarization

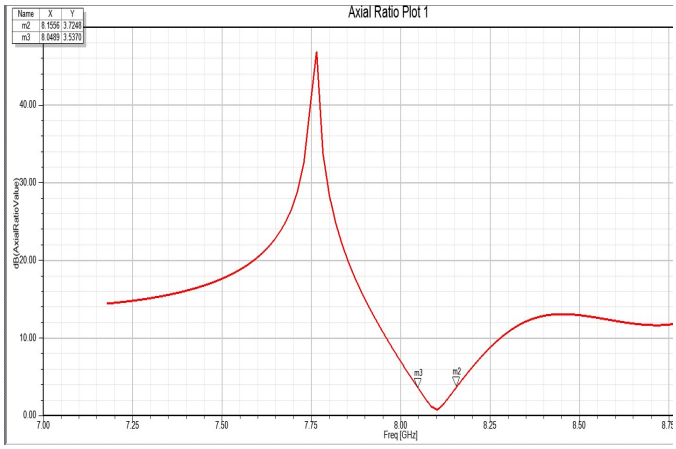

Figure 9. Axial ratio plot in case of circular polarization

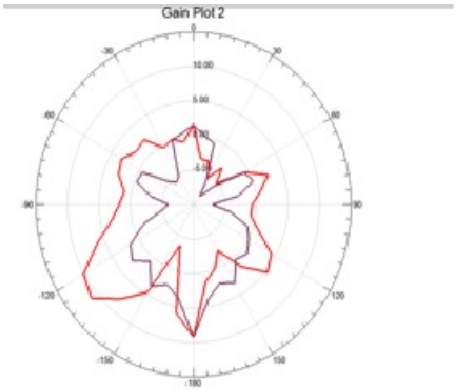

Conclusion

This article introduces a reconfigurable antenna with performance polarization. The design features a primary radiator in the form of a slot antenna. To achieve compact polarization reconfigurability, a Metasurface (MS) is directly positioned on top of the patch antenna. The mechanical rotation of the top MS is employed to reconfigure polarization. The antenna demonstrates effective functionality within the 6GHz to 12 GHz frequency range, converting linear polarization to circular polarization. The validity of the results is confirmed through axial ratio plots. The suggested antenna is applicable in high-frequency scenarios, particularly in Wi-Fi, Wireless LAN, and Wi-Max applications.

[1] A. Mohamed, C. Saha, B. Salim, S. H. Krishna, A. Karthika, V. Megha*, et al.*, "Design of a Graded Index Metasurface Lens for Gain Enhancement of Rectangular Dielectric Resonator Antenna," in *TENCON 2019-2019 IEEE Region 10 Conference (TENCON)*, 2019, pp. 1444-1447.

[2] N. Sood, K. Goodwill, and M. Kartikeyan, "Frequency reconfigurable Fabry Perot cavity antenna using modulated metasurface for WiMAX/WLAN applications," in *2017 IEEE Applied Electromagnetics Conference (AEMC)*, 2017, pp. 1-2.

[3] X. Chen and Y. Zhao, "Dual-band polarization and frequency reconfigurable antenna using double layer metasurface," *AEU-International Journal of Electronics and Communications,* vol. 95, pp. 82-87, 2018.

[4] A. Chen, X. Ning, and L. Wang, "Design of radiation pattern reconfigurable antenna using metasurface," in *2017 International Applied Computational Electromagnetics Society Symposium (ACES)*, 2017, pp. 1-2.

[5] X. Gao, X. Han, W.-P. Cao, H. O. Li, H. F. Ma, and T. J. Cui, "Ultrawideband and high-efficiency linear polarization converter based on double V-shaped metasurface," *IEEE Transactions on Antennas and Propagation,* vol. 63, pp. 3522-3530, 2015.

[6] W. Liu, S. Chen, Z. Li, H. Cheng, P. Yu, J. Li*, et al.*, "Realization of broadband cross-polarization conversion in transmission mode in the terahertz region using a single-layer metasurface," *Optics letters,* vol. 40, pp. 3185-3188, 2015.

[7] H.-X. Xu, S. Sun, S. Tang, S. Ma, Q. He, G.-M. Wang*, et al.*, "Dynamical control on helicity of electromagnetic waves by tunable metasurfaces," *Scientific reports,* vol. 6, pp. 1-10, 2016.

[8] H.-X. Xu, S. Ma, W. Luo, T. Cai, S. Sun, Q. He*, et al.*, "Aberration-free and functionality-switchable meta-lenses based on tunable metasurfaces," *Applied Physics Letters,* vol. 109, p. 193506, 2016.

[9] R. T. Ako, W. S. Lee, M. Bhaskaran, S. Sriram, and W. Withayachumnankul, "Broadband and wide-angle reflective linear polarization converter for terahertz waves," *APL Photonics,* vol. 4, p. 096104, 2019.

[10] W. Ma, G. Wang, B.-f. Zong, Y. Zhuang, and X. Zhang, "Mechanically reconfigurable antenna based on novel metasurface for frequency tuning-range improvement," in *2016 IEEE International Conference on Microwave and Millimeter Wave Technology (ICMMT)*, 2016, pp. 629-631.

[11] C. Ni, M. S. Chen, Z. X. Zhang, and X. L. Wu, "Design of frequency-and polarization-reconfigurable antenna based on the polarization conversion metasurface," *IEEE Antennas and Wireless Propagation Letters,* vol. 17, pp. 78-81, 2017.

[12] H. Zhu, S. Cheung, X. Liu, and T. Yuk, "Design of polarization reconfigurable antenna using metasurface," *IEEE transactions on antennas and propagation,* vol. 62, pp. 2891-2898, 2014.

[13] B. Majumder, K. Krishnamoorthy, J. Mukherjee, and K. Ray, "Frequency-reconfigurable slot antenna enabled by thin anisotropic double layer metasurfaces," *IEEE Transactions on Antennas and Propagation,* vol. 64, pp. 1218-1225, 2016.

[14] M. N. Pavan and N. Chattoraj, "Design and analysis of a frequency reconfigurable antenna using metasurface for wireless applications," in *2015 International Conference on Innovations in Information, Embedded and Communication Systems (ICIIECS)*, 2015, pp. 1-5.

[15] H. Zhu, X. Liu, S. Cheung, and T. Yuk, "Frequency-reconfigurable antenna using metasurface," *IEEE Transactions on Antennas and Propagation,* vol. 62, pp. 80-85, 2013.

[16] J. Qi and Z. Zhang, "Electromagnetic characterization of a metasurface-enabled frequency reconfigurable antenna," in *2016 URSI International Symposium on Electromagnetic Theory (EMTS)*, 2016, pp. 715-717.

[17] M. Zhu and L. Sun, "Design of frequency reconfigurable antenna based on metasurface," in *2017 IEEE 2nd Advanced Information Technology, Electronic and Automation Control Conference (IAEAC)*, 2017, pp. 1785-1788.

[18] H.-X. Xu, T. Cai, Y.-Q. Zhuang, Q. Peng, G.-M. Wang, and J.-G. Liang, "Dual-mode transmissive metasurface and its applications in multibeam transmitarray," *IEEE Transactions on Antennas and Propagation,* vol. 65, pp. 1797-1806, 2017.

[19] H. X. Xu, S. Tang, X. Ling, W. Luo, and L. Zhou, "Flexible control of highly-directive emissions based on bifunctional metasurfaces with low polarization cross-talking," *Annalen der physik,* vol. 529, p. 1700045, 2017.

[20] C. Fang, Y. Cheng, Z. He, J. Zhao, and R. Gong, "Design of a wideband reflective linear polarization converter based on the ladder-shaped structure metasurface," *Optik,* vol. 137, pp. 148-155, 2017.

[21] J. C. Zhao and Y. Z. Cheng, "Ultra-broadband and high-efficiency reflective linear polarization convertor based on planar anisotropic metamaterial in microwave region," *Optik,* vol. 136, pp. 52-57, 2017.

[22] J. Zhao, Y. Cheng, and Z. Cheng, "Design of a photo-excited switchable broadband reflective linear polarization conversion metasurface for terahertz waves," *IEEE Photonics Journal,* vol. 10, pp. 1-10, 2018.

[23] G. Varamini, A. Keshtkar, N. Daryasafar, and M. Naser-Moghadasi, "Microstrip Sierpinski fractal carpet for slot antenna with metamaterial loads for dual-band wireless application," *AEU-International Journal of Electronics and Communications,* vol. 84, pp. 93-99, 2018.

[24] G. Varamini, A. Keshtkar, and M. Naser-Moghadasi, "Miniaturization of microstrip loop antenna for wireless applications based on metamaterial metasurface," *AEU-International Journal of Electronics and Communications,* vol. 83, pp. 32-39, 2018.

[25] H.-X. Xu, S. Tang, G.-M. Wang, T. Cai, W. Huang, Q. He*, et al.*, "Multifunctional microstrip array combining a linear polarizer and focusing metasurface," *IEEE Transactions on Antennas and Propagation,* vol. 64, pp. 3676-3682, 2016.

[26] L.-Y. Ji, P.-Y. Qin, Y. J. Guo, G. Fu, and R. Mittra, "A wideband polarization reconfigurable antenna for WLAN applications," in *2016 10th European Conference on Antennas and Propagation (EuCAP)*, 2016, pp. 1-3.

[27] P. Zhang, Y. Cui, and R. Li, "A novel polarization reconfigurable circularly polarized antenna," in *2017 IEEE International Symposium on Antennas and Propagation & USNC/URSI National Radio Science Meeting*, 2017, pp. 2215-2216.

[28] B. Majumder, K. Kandasamy, J. Mukherjee, and K. Ray, "Dual band dual polarized frequency reconfigurable antenna using meta-surface," in *2015 Asia-Pacific Microwave Conference (APMC)*, 2015, pp. 1-3.

[29] Z. Wu, L. Li, Y. Li, and X. Chen, "Metasurface superstrate antenna with wideband circular polarization for satellite communication

application," *IEEE Antennas and Wireless Propagation Letters,* vol. 15, pp. 374-377, 2015.

[30] Z. Zhang, M. Li, Y. Zhang, D. Li, and M.-C. Tang, "Design of Polarization-Reconfigurable Antenna Based on Hybrid Periodic Metasurface," in *2019 IEEE International Conference on Computational Electromagnetics (ICCEM)*, 2019, pp. 1-3.

[31] A. Chen, X. Ning, L. Wang, and Z. Zhang, "A design of radiation pattern and polarization reconfigurable antenna using metasurface," in *2017 IEEE Asia Pacific Microwave Conference (APMC)*, 2017, pp. 108-111.

[32] H. Gu, J. Wang, and L. Ge, "Circularly polarized patch antenna with frequency reconfiguration," *IEEE Antennas and Wireless Propagation Letters,* vol. 14, pp. 1770-1773, 2015.

[33] G. Feng, C. Guo, and J. Ding, "Frequency-Reconfigurable Slot Antenna Using Metasurface," in *2018 International Conference on Microwave and Millimeter Wave Technology (ICMMT)*, 2018, pp. 1-3.

[34] W. Liu, Z. N. Chen, and X. Qing, "Metamaterial-based low-profile broadband aperture-coupled grid-slotted patch antenna," *IEEE Transactions on Antennas and Propagation,* vol. 63, pp. 3325-3329, 2015.

[35] W. E. Liu, Z. N. Chen, X. Qing, J. Shi, and F. H. Lin, "Miniaturized wideband metasurface antennas," *IEEE Transactions on Antennas and Propagation,* vol. 65, pp. 7345-7349, 2017.

[36] Q. Chen, H. Zhang, Y.-J. Shao, and T. Zhong, "Bandwidth and gain improvement of an L-shaped slot antenna with metamaterial loading," *IEEE Antennas and Wireless Propagation Letters,* vol. 17, pp. 1411-1415, 2018.

[37] F. H. Lin and Z. N. Chen, "Low-profile wideband metasurface antennas using characteristic mode analysis," *IEEE Transactions on Antennas and Propagation,* vol. 65, pp. 1706-1713, 2017.

[38] M. Ameen and R. Chaudhary, "Metamaterial-based wideband circularly polarised antenna with rotated V-shaped metasurface for small satellite applications," *Electronics Letters,* vol. 55, pp. 365-366, 2019.

[39] M. Ameen, O. Ahmad, and R. Chaudhary, "Wideband circularly-polarised high-gain diversity antenna loaded with metasurface reflector for small satellite applications," *Electronics Letters,* vol. 55, pp. 829-831, 2019.

[40] P. Liu, W. Jiang, S. Sun, Y. Xi, and S. Gong, "Broadband and Low-Profile Penta-Polarization Reconfigurable Metamaterial Antenna," *IEEE Access,* vol. 8, pp. 21823-21831, 2020.

[41] Chun Ni, Ming Sheng Chen, Zhong Xiang Zhang, and Xian Liang Wu Design of Frequency and Polarization Reconfigurable Antenna Based on the Polarization Conversion Metasurface, IEEE Antennas and Wireless Propagation Letters